Journal of Applied Pharmaceutical Science Vol. 12(11), pp 021-029, November, 2022
Available online at http://www.japsonline.com
DOI: 10.7324/JAPS.2022.121103
ISSN 2231-3354

In silico approach: Prediction of ADMET, molecular docking, and QSPR of secondary metabolites in Mangroves

Didi Nurhadi Illian[1], Anita Puspa Widiyana[2], Ani Riani Hasana[3], Hilda Maysarah[1], Shofiyah Sabilah Al Mustaniroh[4], Mohammad Basyuni[5*]

[1]Department of Pharmacy, Faculty of Mathematics and Natural Sciences, Universitas Syiah Kuala, Banda Aceh, Indonesia.
[2]Department of Pharmacy, Faculty of Medicine, Universitas Islam Malang, Malang, Indonesia.
[3]Department of Pharmacy, Sekolah Tinggi Ilmu Kesehatan Panti Waluya Malang, Malang, Indonesia.
[4]Department of Mathematics, Faculty of Natural Sciences and Mathematics, Universitas Sumatera Utara, Medan, Indonesia.
[5]Center of Excellence for Mangrove, Universitas Sumatera Utara, Medan, Indonesia.

ARTICLE INFO

Received on: 20/04/2022
Accepted on: 10/07/2022
Available Online: 05/11/2022

Key words:
Emodin, luteolin, dolichol, polyprenol, polyisoprenoids, mangrove, *in silico*.

ABSTRACT

Mangrove plants are known to produce various secondary metabolites (SMs) such as polyisoprenoids (dolichol and polyprenol), emodin, and luteolin to show anticancer, anti-inflammatory, antiviral, and antibacterial activities. This study aimed to predict the multiple activities of the SMs of mangroves based on several enzymes that utilize the *in silico* method. The properties of absorption, distribution, metabolism, excretion, and toxicity for emodin, luteolin, polyprenol C80, dolichol-17 (C85), and dolichol-20 (C100) displayed variation. Prediction for Lipinski's rule showed that emodin and luteolin have lower molecular weight than polyprenol C80, dolichol C85, and dolichol C100. Emodin and luteolin were further docked with cyclooxygenase-2, beta-lactamase, CYP450-dependent 14-alpha demethylase, 3C-like protease, and P-glycoprotein as protein targets using the Molegro Virtual Docker Ver.5.5 approach. In comparison to celecoxib, ketoconazole, clavulanic acid, remdesivir, and verapamil, emodin and luteolin had higher rerank scores. The quantitative structure–property relationships depicted that the electronic parameter, highest occupied molecular orbital (E_{HOMO}), was the physical chemistry parameter that influenced the total clearance. The present findings emphasized that emodin and luteolin from the SMs of mangroves have multiple activities as potent inhibitors of cancer cells and bacterial infections.

INTRODUCTION

Currently, computational designs based on the structure of the target receptors responsible for a compound's toxicity and activity in the body can aid in the discovery of novel drugs. This method of computation is known as "structure-based drug design" or "computer-aided drug design" (CADD) (Song *et al*., 2009). The use of CAAD in finding new drug candidates provides information on the molecular properties of the active compound (Dara *et al*., 2021). Active compounds as ideal new drug candidates have bioavailability (absorption, distribution, metabolism, and elimination) and toxicological data. The value of oral drug absorption depends on the dose, solubility, and permeability according to Lipinski's rule of five. Lipinski's rule of five aims to determine the amount of a compound that is absorbed from the gastrointestinal tract through passive diffusion. The fulfillment of Lipinski's five rules for the active compound shows its solubility in water. Solubility in water is related to faster metabolic processes, elimination time, and side effects of drug accumulation. The appropriate activity test determines if the active compound is sufficiently soluble (Duchowicz *et al*., 2009).

Each active compound has physicochemical properties related to its structure. The predictive use of the chemical properties of the active compound structure has lipophilic, electronic,

*Corresponding Author
Mohammad Basyuni, Center of Excellence for Mangrove, Universitas Sumatera Utara, Medan, Indonesia.
E-mail: m.basyuni @ usu.ac.id

© 2022 Didi Nurhadi Illian *et al*. This is an open access article distributed under the terms of the Creative Commons Attribution 4.0 International License (https://creativecommons.org/licenses/by/4.0/).

and steric parameters. In this study, the quantitative relationship between the structure and chemical properties was determined using the quantitative structure–property relationships (QSPR) model. In addition, the QSPR model can be used to explain chemical properties that affect pharmacokinetic values, especially elimination, which is related to the determination of drug dose values. The elimination parameter used in this study was the total clearance (CL_{TOT}) of the active compound (Praditapuspa *et al*., 2021). The QSPR model has the advantage of being more economical and reducing the need for time-consuming and expensive experiments (Duchowicz *et al*., 2009; Sandfort *et al*., 2020).

The active site of the protein that binds to the drug compound is identified using information from the target protein's structure. Compounds that are expected to bind to the target protein and have biological activity can be designed based on the prediction of the active site. The target protein's structure can be modeled using crystal structure data obtained from databases such as the Protein Data Bank (PDB) or by performing comparative modeling to predict the 3D structure of the unknown target protein based on its similarity (>40% similarity) with the known target protein if the protein structure is not found in the available database. The availability of data is critical to the success of drug discovery and development campaigns (Song *et al*., 2009). Drug development relies heavily on natural products. Natural products have become increasingly popular in pharmacological research during the last 20 years, including in antibacterial medication development. Terpenes, alkaloids, flavonoids, and phenols are only a few of the secondary metabolites (SMs) produced by typical plant metabolic processes that have antibacterial properties. By enhancing membrane permeability, inhibiting enzyme synthesis, or blocking biochemical reactions, natural compounds can address multiple bacterial targets at the same time (Guo *et al*., 2020).

Indonesia is known as the world's most important mangrove area with a diverse range of species (Basyuni *et al*., 2022). Several studies have reported, as presented in Table 1, that mangrove plants contain SMs, i.e., polyisoprenoids (for example, dolichol and polyprenol), anthraquinone (for example, emodin), and flavonoids (for example, luteolin). In addition, they provide properties that are anticancer, anti-inflammatory, antioxidant, antiviral, and antibacterial (Ho *et al*., 2007; Illian *et al*., 2018; 2019, 2021; May Zin *et al*., 2017; Momtazi-Borojeni *et al*., 2013; Odontuya *et al*., 2005; Qurrohman *et al*., 2020; Sumardi *et al*., 2018; Wu *et al*., 2008). The chemical structures of these compounds are shown in Figure 1. Due to the wide-ranging biological activities of polyisoprenoids, anthraquinone, and flavonoids in mangrove plants, these SMs are regarded as potential natural resources for pharmacological and other properties (Table 1). Thus, these observations in concert prompted us to implement the *in silico* method to predict the activities and value of the bond energy between emodin, luteolin, dolichol, and polyprenol on the enzymes of cyclooxygenase-2 (COX-2), beta-lactamase, CYP450-dependent 14-alpha demethylase, 3C-like protease (3CL-pro), and P-glycoprotein (P-GP).

MATERIALS AND METHODS

ADMET prediction

The simplified molecular-input line-entry system series was used to simulate absorption, distribution, metabolism, excretion, and toxicity (ADMET) for emodin, luteolin, di-trans, poly-cis-polyprenol (C80), dolichol-17 (C85), and dolichol-20 (C100) from the SMs of mangrove. The pkCSM (predicting small-molecule pharmacokinetic properties using graph-based signatures) website (Pires *et al*., 2015) was used to determine the properties of emodin, luteolin, di-trans, poly-cis-polyprenol (C80), dolichol-17 (C85), and dolichol-20 (C100). Furthermore, the ProTox-II (prediction of toxicity of chemicals) website was used to predict compounds' toxicity. The predictions of the toxicity chemical class were segmented into the following categories: Class 1 = extremely lethal (lethal dose 50 (LD_{50}) ≤ 5); Class 2 = fatal (5 < LD_{50} ≤ 50); Class 3 = toxic (50 < LD_{50} ≤ 300); Class 4 = harmful (300 < LD_{50} ≤ 2,000); Class 5 = possibly hazardous

Table 1. SMs and their properties from mangrove plants containing polyisoprenoids, emodin, and luteolin.

Mangrove Species	Tissue	[a]SMs	References	Properties	References
Avicennia marina, *Avicennia lanata*, *Avicennia alba*	Leaves	Polyprenol (main C80), Dolichol (main C85), Dolichol (main C100)	(Basyuni *et al*., 2016)	Anticancer activity against WiDr colon cancer cell lines	(Illian *et al*., 2018; Illian *et al*., 2019; Qurrohman *et al*., 2020)
				Antibacterial activity against *E. coli* and *Staphylococcus aureus*	(Sumardi *et al*., 2018)
				Anti-inflammatory and antioxidant activities	(Odontuya *et al*., 2005)
		Luteolin	(Momtazi-Borojeni *et al*, 2013)	An apoptotic agent against MDA-MB-231 human breast cancer cell lines	(Momtazi-Borojeni *et al*, 2013)
Lumnitzera racemosa	Leaves, stems	Emodin	(Wu *et al*., 2008)	Preventing interactions between ACE-2 receptors and the S-protein in SARS-CoV	(Ho *et al*., 2007; Illian *et al*., 2021)
				Moderate antibacterial activity against the Gram-positive bacteria and strong synergistic association with oxacillin against MRSA *Staphylococcus aureus*	(May Zin *et al*., 2017)

[a]SMs, Secondary metabolites.

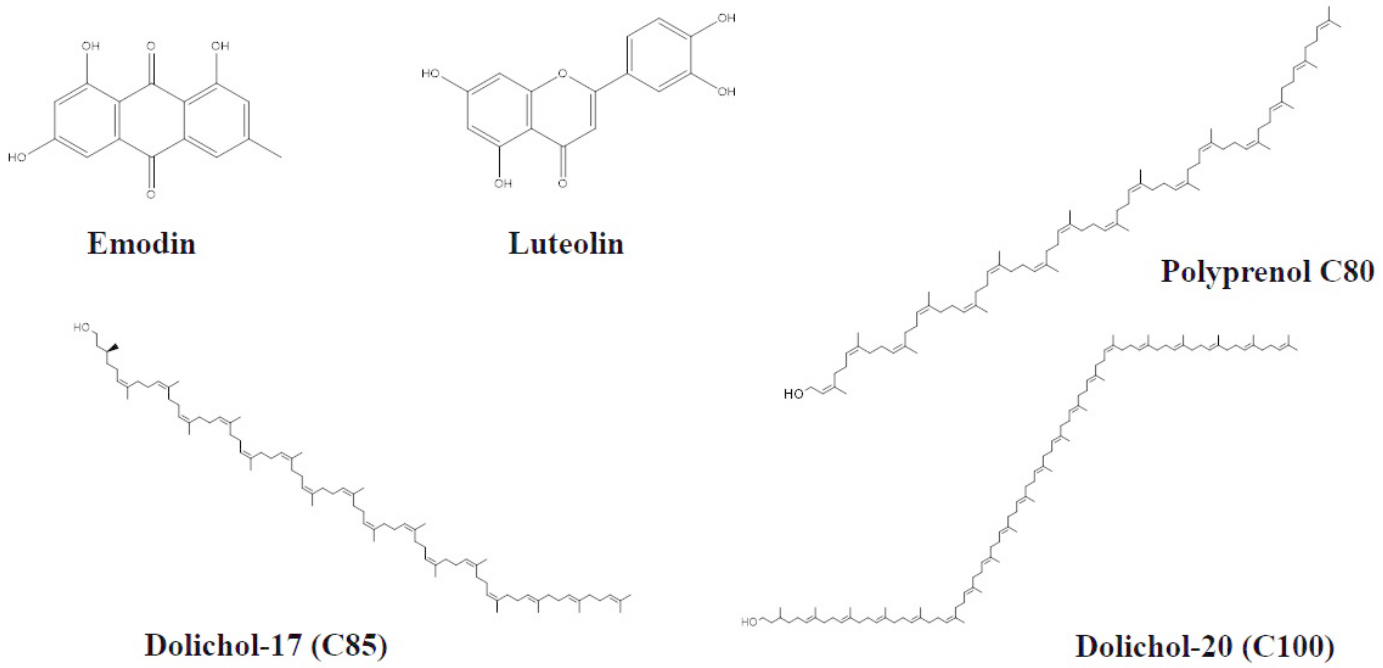

Figure 1. The 2D chemical structure of secondary metabolites from mangrove plants used in this study: emodin, luteolin, polyprenol C80, dolichol-17 (C85), and dolichol-20 (C100).

(2,000 < LD_{50} ≤ 5,000); and Class 6 = nontoxic (LD_{50} > 5,000) (OECD, 2001).

Prediction for Lipinski's rule of five

According to "the rule of five" in the discovery setting, when there are more than 5 H-bond donors and 10 H-bond acceptors, the molecular weight surpasses 500, and when the computed LogP surpasses 5, it is more likely that there will be poor absorption or penetration (Lipinski, 2004). The physicochemical parameters were predicted by the ChemBio 3D Ultra ver.13 software.

Determination of QSPR

The determination of QSPR aimed to determine the quantitative relationship between the structure and physicochemical parameters (Shoombuatong *et al*., 2017). The physicochemical parameters included the lipophilic, electronic, and steric parameters. The lipophilic parameters included LogP and LogS. The electronic parameters included E_{TOT}, E_{HOMO}, and E_{LUMO}. The steric parameters included molecular weight and molecular volume. The prediction of CL_{TOT} value as a parameter of drug elimination was made by pkCSM. SPSS ver. 26 was used for the determination of the QSPR equation.

Preparation for the X-ray structure of the target protein

The protein targets were human COX-2 (PDB ID: 3LN1), beta-lactamase (PDB ID: 1LLB, 6W33), CYP450-dependent 14-alpha demethylase (PDB ID: 1JIP), 3CL-pro (PDB ID: 6LU7), and P-GP (PDB ID: 1MV5, 4DGN), which were obtained from the Protein Data Bank (PDB) website [Research Collaboratory for Structural Bioinformatics (RCSB) PDB].

Preparation of ligands

ChemBioDraw Ultra ver. 13.0 (Cambridge Soft) was used to draw the structures of emodin and luteolin. ChemBio 3D 13.0 was used to convert the compound's 2D structures to 3D structures. The Merck molecular force field (MMFF94) method was used to optimize the molecule and minimize the geometry of the ligand, and the results were saved in SYBYL.mol2 format, which the Molegro Virtual Docker (MVD) software could read.

Molecular docking studies

Molecular docking techniques on MVD Ver. 5.5 (CLC Bio) were used to investigate the activities of emodin and luteolin on COX-2, beta-lactamase, CYP450-dependent 14-alpha demethylase, and P-GP interaction. Human COX-2 (code 3LN1), beta-lactamase (code 1LLB, 6W33), CYP450-dependent 14-alpha demethylase (code 1JIP), 3CL-pro (code 6LU7), and P-GP (code 1MV5, 4DGN) crystal structures were used as protein targets. To get the docked posture and root mean square deviation (RMSD), the docking process was validated by redocking the ligands of 3LN1 (Wang *et al*., 2010), 1LLB (Trehan *et al*., 2002), 6LU7 (Jin *et al*., 2020), 6W33, 1JIP (Cupp-Vickery *et al*., 2001), 1MV5, and 4DGN (Lolli *et al*., 2012) into its binding pocket within the crystals of COX-2, beta-lactamase, CYP450-dependent 14-alpha demethylase, and P-GP. The protocol is effective at recreating the X-ray crystal structure in complex forms for further docking investigations.

RESULTS AND DISCUSSION

ADMET prediction

The properties of ADMET for emodin, luteolin, di-trans, poly-cis-polyprenol (C80), dolichol-17 (C85), and dolichol-20 (C100) are presented in Table 2 based on the computational analysis using pkCSM. In addition, the toxicity class predictions for emodin, luteolin, polyprenol C80, dolichol-17 (C85), and dolichol-20 (C100) are presented in Table 3.

The pharmacokinetic data in Table 2 revealed that emodin and dolichol-20 (C100) do not inhibit CYP3A4 enzymes, suggesting that it is safe to use emodin and dolichol-20 (C100) with a wide range of CYP3A4 substrates (including alprazolam, atorvastatin, vincristine, halothane, hydrocortisone, zidovudine, carbamazepine, codeine, cortisol, caffeine, lidocaine, lovastatin, midazolam, nifedipine, paracetamol, tacrolimus, tamoxifen, testosterone, phenytoin, cyclosporine, cyclophosphamide, erythromycin, R-warfarin, and S-warfarin). This is due to the fact that the isoenzyme type CYP3A4 is the primary metabolizer of approximately 75% of all medicines metabolized by CYP (Zhang *et al*., 2021). According to a prior study examining the 200 most widely prescribed medications in the United States, the CYP isoenzyme

Table 2. The properties of ADMET: emodin, luteolin, di-trans, poly-cis-polyprenol (C80), dolichol-17 (C85), and dolichol-20 (C100)

Properties	Emodin	Luteolin	di-trans,poly-cis-polyprenol (C80)	dolichol-17 (C85)	dolichol-20 (C100)	Unit
Absorption						
Water solubility	−3.19	−3.09	−2.89	−2.89	−2.89	Numeric (log mol/l)
Caco2 permeability	0.06	0.10	1.08	1.24	1.25	Numeric (log Papp in 10^{-6} cm/s)
Intestinal absorption (human)	74.49	81.13	75.19	83.98	82.21	Numeric (% Absorbed)
Skin permeability	−2.74	−2.74	−2.74	−2.74	−2.74	Numeric (log Kp)
P-glycoprotein substrate	Yes	Yes	No	No	No	Categorical (Yes/No)
P-glycoprotein I inhibitor	No	No	No	No	No	Categorical (Yes/No)
P-glycoprotein II inhibitor	No	No	Yes	Yes	Yes	Categorical (Yes/No)
Distribution						
VDss (human)	0.46	1.15	−0.21	−0.22	−0.05	Numeric (log L/kg)
Fraction unbound (human)	0.18	0.17	0.37	0.37	0.38	Numeric (Fu)
BBB permeability	−0.73	−0.91	1.37	1.59	1.78	Numeric (log BB)
CNS permeability	−2.34	−2.25	1.00	1.06	1.72	Numeric (log PS)
Metabolism						
CYP2D6 substrate	No	No	No	No	No	Categorical (Yes/No)
CYP3A4 substrate	No	No	Yes	Yes	Yes	Categorical (Yes/No)
CYP1A2 inhibitor	Yes	Yes	No	No	No	Categorical (Yes/No)
CYP2C19 inhibitor	No	No	No	No	No	Categorical (Yes/No)
CYP2C9 inhibitor	No	Yes	No	No	No	Categorical (Yes/No)
CYP2D6 inhibitor	No	No	No	No	No	Categorical (Yes/No)
CYP3A4 inhibitor	No	No	No	No	No	Categorical (Yes/No)
Excretion						
Total clearance	0.34	0.50	1.84	1.81	1.75	Numeric (log ml/min/kg)
Renal OCT2 substrate	No	No	No	No	No	Categorical (Yes/No)
Toxicity						
AMES toxicity	No	No	No	No	No	Categorical (Yes/No)
Max. tolerated dose (human)	0.16	0.50	0.44	0.44	0.44	Numeric (log mg/kg/day)
hERG I inhibitor	No	No	No	No	No	Categorical (Yes/No)
hERG II inhibitor	No	No	Yes	Yes	Yes	Categorical (Yes/No)
Oral rat acute toxicity (LD50)	2.12	2.46	2.52	2.52	2.49	Numeric (mol/kg)
Oral rat chronic toxicity (LOAEL)	2.07	2.41	−0.69	−0.73	−1.14	Numeric (log mg/kg_bw/day)
Hepatotoxicity	No	No	No	No	No	Categorical (Yes/No)
Skin sensitization	No	No	No	No	No	Categorical (Yes/No)
T. pyriformis toxicity	0.54	0.33	0.29	0.29	0.29	Numeric (log ug/L)
Minnow toxicity	2.06	3.17	−12.24	−15.06	−18.26	Numeric (log mM)

Table 3. The toxicity prediction of emodin, luteolin, di-trans, poly-cis-polyprenol (C80), dolichol-17 (C85), and dolichol-20 (C100).

Parameters	Emodin	Luteolin	di-trans, poly-cis-polyprenol (C80)	Dolichol-17 (C85)	Dolichol-20 (C100)
Predicted LD_{50}	5,000 mg/kg	3,919 mg/kg	1,190 mg/kg	5,600 mg/kg	5,600 mg/kg
Predicted toxicity class	Class 5	Class 5	Class 4	Class 6	Class 6
Average similarity	80.50%	80.53%	100.00%	87.37%	87.37%
Prediction accuracy	70.97%	70.97%	100.00%	70.97%	70.97%

type CYP3A4 metabolizes around 46% of pharmaceuticals (Sychev *et al*., 2018).

Another pharmacokinetic predictor is toxicity. Based on the Ames test toxicity data, it is known that the five compounds are not mutagenic, skin-sensitizing, or hepatotoxic. Emodin and luteolin compounds are not inhibitors of *hERG I* or *hERG II* associated with potassium channels. Meanwhile, polyprenol (C80) and dolichol (C85 and C100) compounds are seen from the inhibition parameters of *hERG* (the human Eth-er-ago-go-related). These three compounds are known to inhibit *hERG II*. *hERG* is a gene that encodes a protein potassium channel that contributes to heart rate activity. Other parameters, such as the maximum tolerated dose, LD_{50}, and LOAEL values, can be classified as good and having a low maximum tolerance dose. However, these five compounds are known to be toxic to *Tetrahymena pyriformis* (Fadlan *et al*., 2021).

Based on Table 3, which presents the details about the toxicity class prediction of emodin, luteolin, di-trans,poly-cis-polyprenol (C80), dolichol-17 (C85), and dolichol-20 (C100), it was observed that emodin was categorized as Class 5 = possibly hazardous ($2{,}000 < LD_{50} \leq 5{,}000$), luteolin was Class 5 = possibly hazardous ($2{,}000 < LD_{50} \leq 5{,}000$), di-trans,poly-cis-polyprenol (C80) was Class 4 = harmful ($300 < LD_{50} \leq 2{,}000$), dolichol-17 (C85) as Class 6 = nontoxic ($LD_{50} > 5{,}000$), and dolichol-20 (C100) as Class 6 = nontoxic ($LD_{50} > 5{,}000$). The LD_{50} value is a standard for determining acute toxicity in mg of compound per kg of body weight. The LD_{50} value, according to Walum (1998), is the dose required to kill 50% of the experimental animal population. The lower the LD_{50} dose, the more hazardous the compound. According to Lipinski's rule of five, emodin and luteolin compounds were easier to absorb and had higher permeability than compounds of di-trans, poly-cis-polyprenol (C80), dolichol-17 (C85), and dolichol-20 (C100) (Lipinski, 2004).

Prediction for Lipinski's rule of five

Table 4 shows that emodin and luteolin have lower molecular weights of 270.24 and 286.24 g/mol, respectively, than di-trans, poly-cis-polyprenol (C80), dolichol-17 (C85), and dolichol-20 (C100), which have molecular weights of 1,107.92, 1,178.05, and 1,382.41 g/mol, respectively. These data suggested that di-trans, poly-cis-polyprenol (C80), dolichol-17 (C85), and dolichol-20 (C100) compounds failed to meet Lipinski's rule of five. The LogP revealed that compounds of emodin (1.51) and luteolin (0.77) meet Lipinski's rule of five requirements. The number of hydrogen bond acceptors (HBA) in emodin and luteolin compounds was 5 and 6, respectively, indicating that they satisfied Lipinski's five-requirement criterion. Emodin and luteolin compounds had three and four hydrogen bond donors, respectively, demonstrating that they met Lipinski's rule of five requirements.

Determination of QSPR

One of the seven regression equations with the best correlation coefficient and significance was chosen (see Table 5). The following was considered the best regression equation for the review (Widiyana *et al*., 2016):

$$1/CL_{TOT} = 0.255\ E_{HOMO} + 3.110.$$

$$(n = 5,\ R = 0.985,\ SE = 0.071,\ F = 95.555,\ sig = 0.002) \quad (1)$$

The equation was chosen since it has the best correlation coefficient ($R = 0.985$), the smallest significance of 0.002 (<0.05), the smallest standard error (SE = 0.071), and the largest F-value (95.555). The physical chemistry parameter that affected the CL_{TOT}, according to the equation, was the electronic parameter E_{HOMO} (as shown in Tables 5 and 6).

Molecular docking studies

Emodin and luteolin were further docked with beta-lactamase, CYP450-dependent 14-alpha demethylase, COX-2, 3CL-pro, and P-GP as protein targets using the MVD Ver. 5.5 docking simulation approach (Widiyana *et al*., 2021). Based on two criteria, such as ligand-binding position and fitness function score comparison, this algorithm determined the best docking score. The RMSD was used to determine the most optimal ligand-binding location. Table 7 presents the interactions of emodin and luteolin with COX-2, beta-lactamase, CYP450-dependent 14-alpha demethylase, 3CL-pro, and P-GP.

Molecular docking is a computer simulation of a ligand binding to a receptor that aids in predicting the protein target (in which the molecule will form a bond) and assessment of the binding affinity. Furthermore, the pose organizer can rotate the hydrogen molecules in both the receptor and the ligand to their ideal position. It is also possible to utilize it to rerank the ligands (using a rank score). The middle panel enables the recalculation of scoring functions, including the MolDock score, binding affinity score, and reranking score, while analyzing docking data. If the poses are imported from an MVD results file, these scoring function values have already been computed. Recalculating the scores for each of the three metrics is done by pressing the "recalculate energies" button (using the coefficients specified in the files for the binding affinity and reranking scores). Using a more computationally sophisticated scoring algorithm than the one used during docking, it is feasible to rerank poses. Numerous components (such as van der Waals forces, electrostatic interactions, and solvent terms) can be manually adjusted in this reranking score function. In MVD, the MolDock, MolDock GRID, and rerank scores are not expressed in chemically meaningful units. However, the MVD can provide an approximation estimate of the binding affinity (Piramanayagam and Lisina, 2014).

Table 4. Prediction for Lipinski's rule of five.

Rules	Emodin	Luteolin	di-trans, poly-cis-polyprenol (C80)	Dolichol-17 (C85)	Dolichol-20 (C100)
MW < 500	270.24	286.24	1,107.92	1,178.05	1,382.41
Hydrogen bond donors < 5	3	4	1	1	1
HBA < 10	5	6	1	1	1
LogP < 5	1.51	0.77	19.79	21.92	25.70

Table 5. Regression analysis between physical and chemical properties with $1/CL_{TOT.}$

No.	Independent Variable	*R*	SE	*F*	Sig.	Equation
1	LogP	0.962	0.112	36.932	0.009	$1/CL_{TOT}$ = −0.029 LogP + 0.403
2	LogS	0.961	0.114	35.985	0.009	$1/CL_{TOT}$ = 0.038 LogS + 0.476
3	E_{TOT}	0.959	0.116	34.499	0.010	$1/CL_{TOT}$ = −0.002 E_{TOT} + 0.439
4	E_{HOMO}	0.985	0.071	95.555	0.002	$1/CL_{TOT}$ = 0.255 E_{HOMO} + 3.110
5	E_{LUMO}	0.611	0.324	1.791	0.273	$1/CL_{TOT}$ = −0.015 E_{LUMO} + 0.060
6	MW	0.713	0.287	3.111	0.176	$1/CL_{TOT}$ = 2.173 10^{-5} MW − 0.113
7	MR	0.982	0.078	79.668	0.003	$1/CL_{TOT}$ = 0.009 MR − 0.252

Table 6. Data of chemical descriptor.

Compounds	Lipophilic		Electronic			Steric		$^{h}CL_{TOT}$	Log (1/CL_{TOT})
	[a]LogP	[b]LogS	$^{c}E_{TOT}$	$^{d}E_{HOMO}$	$^{e}E_{LUMO}$	[f]MW	[g]MR		
Emodin	1.51	–2.96	33.53	–10.30	–7.33	270.24	71.28	0.34	0.47
Luteolin	0.77	–2.75	29.96	–11.20	–3.83	286.24	73.53	0.50	0.30
di-trans,poly-cis-polyprenol (C80)	19.79	–16.90	282.80	–13.03	0.62	1107.92	0	1.84	–0.26
Dolichol-17 (C85)	21.92	–18.53	269.09	–12.98	0.29	1178.05	0	1.81	–0.26
Dolichol-20 (C100)	25.70	–21.80	348.88	–13.47	0.88	1382.41	0	1.75	–0.24

[a]LogP: Partition coefficient, [b]LogS: Solubility, $^{c}E_{TOT}$: Minimum energy (kcal/mol), $^{d}E_{HOMO}$: Highest occupied molecular orbital (eV), $^{e}E_{LUMO}$: Lowest unoccupied molecular orbital (eV), [f]MW: Molecular weight (g/mol), [g]MR: Molar refractivity (cm^3/mol), $^{h}CL_{TOT}$: Clearance total (log ml/minute/kg).

Table 7. The binding energy of emodin and luteolin.

Activities	Mechanism of action	PDB-ID	Re-rank score		
			Standard	Emodin	Luteolin
Antibacterial	Beta-lactamase inhibitor	1LLB	Clavulanic acid	−74.04	−85.78	−88.47
		6W33		−79.53	71.18	−82.83
Antifungal	CYP450-dependent 14-alpha demethylase inhibitor	1JIP	Ketoconazole	−135.08	−71.62	−73.81
Anti-inflammatory	COX-2 inhibitor	3LN1	Celecoxib	−137.80	−85.02	−106.84
Antiviral	3CL-pro inhibitor	6LU7	Remdesivir	−128.35	−83.99	−96.22
Anticancer	P-GP inhibitor	1MV5	Verapamil	−74.28	−77.94	−73.94
		4DGN		−80.97	−92.56	−101.57

In numerous types of activity, the proteins mentioned above are shown to be overexpressed. Since the target molecules' X-ray crystallographic structures are known, structure-based rational drug design methodologies can be used to build novel lead compounds based on them. The active site of the target compounds was discovered and molecular docking was performed using ChemBio 3D 13.0 containing 3D structures of chemicals obtained from marine systems. MVD handles every step of the docking procedure, from preparing the compounds to determining the target protein's probable binding sites and predicting the ligands' binding modes. MVD provides high-quality docking by combining a revolutionary optimization technique with a user interface that prioritizes usability and efficiency. The computational experiment yielded the identification of a 5-second metabolite that docked perfectly into the target's active site. For each ligand, a visual evaluation of the top-ranking molecules (hits) generated a list of roughly five small molecules. The docked postures were listed along with the rerank scores that correlate with them. The

MolDock score calculated for "hits" was significantly higher than the MolDock score calculated for the original ligand–protein docking. According to the energy principle, the lowest score was used since a molecule is most stable at the lowest energy level. As a result, it was worthwhile to test the actual binding affinities of these small molecules to the target protein to see if the computer predictions corresponded to the biological scenario (Widiyana, 2021; Zhang *et al*., 2021).

The receptor structure used in this study was obtained from the Research Collaboratory for Structural Bioinformatics (RCSB) PDB. Each protein provides information about the active site and the composition of the secondary metabolite–protein binding space as well as the opportunity to use the enzyme or protein in a functional conformation. In the current investigation, we tested five activities, including antibacterial activity with a beta-lactamase inhibitor mechanism, antifungal activity with a CYP450-dependent 14-alpha demethylase inhibitor mechanism, anti-inflammation activity with a COX-2 inhibitor mechanism, antiviral activity with a 3CL-pro inhibitor mechanism, and anticancer activity with a P-GP inhibitor mechanism (Puspaningtyas, 2013). The validation stage was carried out to calibrate the docking method *in silico* by repeating the prediction of the native ligand's binding ability to proteins and then comparing it with the position of the original native ligand, which is innate to the receptor on the ligand-binding site pocket. The assessment parameter used to provide an assessment of validity was the RMSD value. The RMSD value was close to zero, indicating that the position of the copy ligand after the superimposition was approaching that of the native ligand, implying that the method utilized would be more precise. Validation was carried out at the pocket ligand-binding site with 10 replications. To ensure that the orientation of the ligand matches the behavior in the ligand–receptor binding model and the position obtained from the docking study using the MVD program, the parameters of this docking method first needed to be validated by the structure of the receptor used, namely PDB, which was replicated 10 times. The rerank score is a value that represents the binding energy required to form a bond between the ligand and the receptor, and it predicts compound activity. It also improves the ligand–receptor interaction. Emodin and luteolin were docked as ligands with COX-2, beta-lactamase, CYP450-dependent 14-alpha demethylase, 3CL-pro, and P-GP as protein targets using the MVD Ver. 5.5 docking simulation approach. This algorithm determined the best docking score based on two criteria: ligand-binding position and fitness function score comparison. The lower value of the rerank indicated the strength of the ligand–receptor bond. The most optimal ligand-binding location was determined using the RMSD.

Docking analysis was performed for antibacterial activity using the mechanism of inhibition toward beta-lactamase using PDB code 1LLB, which contains the inhibitor crystal structure of AmpC beta-lactamase from *Escherichia coli* in a complex with ATMO-penicillin (https://www.rcsb.org/structure/1llb), and PDB code 6W33, which contains the crystal structure of Class A beta-lactamase from *Bacillus cereus* in a complex with the beta-lactamase inhibitor of clavulanate acid (https://www.rcsb.org/structure/6W33). At this point, the test compounds' interactions with the 1LLB and 6W33 receptors were compared to interaction with clavulanic acid as the standard. Interactions with the 1LLB receptor had a higher rerank score of −74.04 than interaction with clavulanic acid (as presented in Table 7), and since emodin and luteolin had the lowest rerank scores (−85.78 and −88.47 kcal/mol, respectively), this indicated that emodin and luteolin have higher binding energies than the others. Furthermore, interaction with the 6W33 receptor had a higher rerank score of −79.53 than interaction with clavulanic acid (see Table 7), and since luteolin had the lowest rerank score (−82.83 kcal/mol), luteolin revealed higher binding energies than the others. These results predicted that emodin and luteolin might have antibacterial activity and are related to overcoming beta-lactamase enzyme-mediated multidrug resistance through the mechanism of beta-lactamase inhibition.

Docking analysis was carried out for antifungal activity using the mechanism of inhibition toward CYP450-dependent 14-alpha demethylase (PDB code 1JIP), which contains keto-conazole-induced conformational changes in the active site of cytochrome mammalian P450 enzymes (https://www.rcsb.org/structure/1JIP). At this point, the test compounds' interactions with the 1JIP receptor were compared to interaction with ketoconazole as the standard. Interaction with the 1JIP receptor in comparison to interaction with ketoconazole had a higher rerank score of −135.08 (see Table 7), and since emodin and luteolin had the lowest rerank scores (−71.62 and −73.81 kcal/mol, respectively), emodin and luteolin exhibited lower binding energies than the others. These results predicted that emodin and luteolin might lack antifungal activity through the mechanism of CYP450 inhibition. Further investigation into the antifungal activity of emodin and luteolin using the other mechanisms is needed.

Docking analysis was carried out for anti-inflammation activity using the mechanism of inhibition toward COX-2 (PDB code 3LN1), which contains the structure of celecoxib bound at the COX-2 inhibitor active site (https://www.rcsb.org/structure/3LN1). At this point, the test compounds' interactions with the 3LN1 receptor were compared to interaction with celecoxib as the standard. Interaction with the 3LN1 receptor had a higher rerank score of −137.80 than interaction with celecoxib (see Table 7), and since emodin and luteolin had the lowest rerank scores (−85.02 and −106.84 kcal/mol, respectively), emodin and luteolin exhibited lower binding energies than the others. These results predicted that emodin and luteolin might lack anti-inflammatory activity through the mechanism of COX-2 inhibition (Park *et al*., 2016). Further investigation into the anti-inflammatory activity of emodin and luteolin using the other mechanisms is needed.

Docking analysis was carried out for antiviral activity using the mechanism of inhibition toward the 3CL-pro inhibitor (PDB code 6LU7), which contains the crystal structure of COVID-19 main protease in a complex with an inhibitor N3 (https://www.rcsb.org/structure/6LU7). At this point, the test compounds' interactions with the 6LU7 receptor were compared to interaction with remdesivir as the standard. Interaction with the 6LU7 receptor in comparison to interaction with remdesivir had a higher rerank score of −128.35 (see Table 7), and since emodin and luteolin had the lowest rerank scores (−83.99 and −96.22 kcal/mol, respectively), emodin and luteolin exhibited lower binding energies than the others. These results predicted that emodin and luteolin might lack antiviral activity against SARS-CoV-2 through the mechanism of 3CL-pro inhibition (Mandal *et al*., 2021). Further investigation into the antiviral activity of emodin and luteolin using the other mechanisms is needed.

Docking analysis was carried out for anticancer activity using the mechanism of inhibition toward P-GP using PDB code 1MV5, which contains the crystal structure of the LmrA ATP-binding domain (https://www.rcsb.org/structure/1mv5), and PDB code 4DGN, which contains the crystal structure of maize CK2 in a complex with the inhibitor luteolin (https://www.rcsb.org/structure/4dgn). At this point, the test compounds' interactions with the 1MV5 and 4DGN receptors were compared to interaction with verapamil as the standard. Interaction with the 1MV5 receptor had a higher rerank score of −74.28 (see Table 7) than interaction with verapamil, and since emodin had the lowest rerank score (−77.94), emodin exhibited higher binding energies than the others. However, luteolin, which had a rerank score of −73.94, can show anticancer activity since it has a value similar to the rerank score of verapamil. Furthermore, interaction with the 4DGN receptor had a higher rerank score of −80.97 (see Table 7) than verapamil, and since emodin and luteolin had the lowest rerank scores (−92.56 and −101.57 kcal/mol, respectively), emodin and luteolin exhibited higher binding energies than the others. These results predicted that emodin and luteolin might show anticancer activity and are related to overcoming P-GP-mediated multidrug resistance through the mechanism of P-GP inhibition.

CONCLUSION

The present study suggested that emodin and luteolin have lower toxicity than the standard, while the standard has a higher affinity for protein enzymes than emodin and luteolin. The findings emphasized that these compounds may show multiple activities as potent inhibitors of cancer cells as well as bacterial infections. Therefore, for further investigation to ascertain the effectiveness against cancer cells and bacterial infections as well as fungal and viral infections, synthesis and *in vitro* evaluation are required.

AUTHORS' CONTRIBUTIONS

DNI, APW, and MB contributed to conceptualization; APW, ARH, DNI, HM, and MB contributed to methodology; ARH and APW used the software; APW, ARH, SSAM, and DNI contributed to validation; MB collected the resources; DNI contributed to original draft preparation; DNI, APW, ARH, HM, SSAM, and MB contributed to review and editing; MB supervised the study; MB contributed to funding acquisition. All authors have read and agreed to the published version of the manuscript.

FUNDING

This research and article processing charge (APC) was funded by a research grant from the Indonesian Science Fund and the Indonesia Endowment Fund for Education (DIPI/LPDP-UKRI Joint Call, Grant Number No. NE/P014127.1).

CONFLICTS OF INTEREST

The authors declare no conflicts of interest.

ETHICAL APPROVAL

This is not applicable. This study does not involve experiments on animals or human subjects.

DATA AVAILABILITY

No additional data is available for this paper.

PUBLISHER'S NOTE

This journal remains neutral with regard to jurisdictional claims in the published institutional affiliation.

REFERENCES

Basyuni M, Sagami H, Baba S, Iwasaki H, Oku H. Diversity of polyisoprenoids in ten Okinawan Mangroves. Dendrobiology, 2016; 75:167–75; doi:10.12657/denbio.075.016

Basyuni M, Sasmito SD, Analuddin K, Ulqodry TZ, Saragi-Sasmito MF, Eddy S, Milantara N. Mangrove Biodiversity, Conservation and Roles for Livelihoods in Indonesia. In: Das SC, Pullaiah T, Ashton EC. (eds) Mangroves: Biodiversity, Livelihoods and Conservation, 2022; 397-445. Springer Nature Singapore Pte Ltd, Singapore; doi:10.1007/978-981-19-0519-3_16

Cupp-Vickery JR, Garcia C,Hofacre A, McGee-Estrada K. Ketoconazole-induced conformational changes in the active site of cytochrome P450eryF. J Mol Biol, 2001: 311:101–10; doi:10.1006/jmbi.2001.4803

Dara S, Dhamercherla S, Jadav SS, Babu CM, Ahsan MJ. Machine learning in drug discovery: a review. Artif Intell Rev, 2021; doi:10.1007/s10462-021-10058-4.

Duchowicz PR, Castro EA. QSPR studies on aqueous solubilities of drug-like compounds. Int J Mol Sci, 2009; 10:2558–77.

Fadlan A, Warsito T. Pendekatan In silico dalam Menyingkap Potensi Antikanker Meciadanol. Jurnal Kimia Riset, 2021: 6(2):163–71.

Guo Y, Liu Y, Zhang Z, Chen M, Zhang D, Tian C, Liu M, Jiang G. The antibacterial activity and mechanism of action of Luteolin against *Trueperella pyogenes*. Infect Drug Resist, 2020; 13:1697–711; doi:10.2147/IDR.S253363

Ho TY, Wu SL, Chen JC, Li CC, Hsiang CY. Emodin blocks the SARS coronavirus spike protein and angiotensin-converting enzyme 2 interaction. Antiviral Res, 2007; 74(2):92–101.

Illian DN, Basyuni M, Wati R, Hasibuan PAZ. Polyisoprenoids from *Avicennia marina* and *Avicennia lanata* inhibit WiDr cells proliferation. Pharmacogn Magazine, 2018; 14:513–8; doi:10.4103/pm.pm_201_18

Illian DN, Hasibuan PAZ, Sumardi S, Nuryawan A,Wati R, Basyuni M. Anticancer activity of polyisoprenoids from *Avicennia alba* Blume. In WiDr Cells. Iranian J Pharm Res, 2019; 18:1477–87; doi:10.22037/ijpr.2019.1100719

Illian DN, Siregar ES, Sumaiyah S, Utomo AR, Nuryawan A, Basyuni M. Potential compounds from several Indonesian plants to prevent SARS-CoV-2 infection: a mini-review of SARS-CoV-2 therapeutic targets. Heliyon, 2021; 7.

Jin Z, Du X, Xu Y, Deng Y, Liu M, Zhao Y, Zhang B, Li X, Zhang L, Peng C, Duan Y, Yu J, Wang L, Yang K, Liu F, Jiang R, Yang X, You T, Liu X, Yang X, Bai F, Liu H, Liu X, Guddat LW, Xu W, Xiao G, Qin C, Shi Z, Jiang H, Rao Z, Yang H. Structure of Mpro from SARS-CoV-2 and dis-covery of its inhibitors. Nature, 2020; 582(7811):289–93, doi.org/10.1038/s41586-020-2223-y.

Lipinski CA. Lead- and drug-like compounds: the rule-of-five revolution. Drug Discov Today Technol, 2004; 1:337–41.

Lolli G, Cozza G, Mazzorana M, Tibaldi E, Cesaro L, Donella-Deana A, Meggio F, Venerando A, Franchin C, Sarno S, Battistutta R, Pinna LA. Inhibition of protein kinase CK2 by flavonoids and tyrphostins. a structural insight. Biochemistry, 2012; 51:6097–107; doi:10.1021/bi300531c

Mandal A, Jha AK, Hazra B. Plant products as inhibitors of coronavirus 3CL protease. Front Pharmacol, 2021; 12; doi:10.3389/fpar.2021.583387

May Zin WW, Buttachon S, Dethoup T, Pereira JA, Gales L, Inácio Â, Costa PM, Lee M, Sekeroglu N, Silva AMS, Pinto MMM, Kijjoa A. Antibacterial and antibiofilm activities of the metabolites isolated from the culture of the Mangrove-derived endophytic fungus Eurotium Chevalieri KUFA 0006. Phytochemistry, 2017; 141:86–97; doi:10.1016/j.phytochem.2017.05.015

Momtazi-Borojeni AA, Behbahani M, Sadeghi-aliabadi H. Antiproliferative activity and apoptosis induction of crude extract and fractions of *Avicennia Marina*. Iran J Basic Med Sci, 2013; 16.

Odontuya G, Hoult JRS, Houghton PJ. Structure activity relationship for antiinflammatory effect of luteolin and its derived glycosides. Phytother Res, 2005; 19:782–6.

OECD Organisation for Economic Co-Operation and Development (OECD). Guideline for testing of chemicals, OECD, Paris, France, 2001.

Park SY, Jin ML, Ko MJ, Park G, Choi Y-W. Anti-neuroinflammatory effect of emodin in LPS-stimulated microglia: involvement of AMPK/Nrf2 activation. Neurochem Res, 2016; 41:2981–92; doi:10.1007/s11064-016-2018-6

Piramanayagam S, Lisina KV. An in silico study on anti inflammatory compounds from marine system using Molegro Virtual Docker. World J Pharm Sci, 2014; 2(4):283–93.

Pires DEV, Blundell TL, Ascher DB. pkCSM: predicting small-molecule pharmacokinetic and toxicity properties using graph-based signatures. J Med Chem, 2015; 58(9):4066–72; doi: 10.1021/acs.jmedchem.5b00104

Praditapuspa EN, Siswandono, Widiandani T. In silico analysis of pinostrobin derivatives from *Boesenbergia pandurata* on ErbB4 kinase target and QSPR linear models to predict drug clearance for searching anti-breast cancer drug candidates. Pharmacogn J, 2021; 13:1143–9; doi:10.5530/pj.2021.13.147

Puspaningtyas AR. Docking Molekul dengan Metoda Molegro Virtual Docker dari Ekstrak Air Psidium Guajava, Linn dan Citrus Sinensis, Peels sebagai Inhibitor pada Tirosinase untuk Pemutih Kulit. Jurnal Kimia Terapan Indonesia, 2013; 15:31–9; doi:10.14203/jkti.v15i1.102

Qurrohman T, Basyuni M, Hasibuan PAZ. Polyisoprenoids from Avicennia marina induces on P13k, Akt1, Mammalian target of rapamycin, Egfr, and P53 gene expression using reverse transcription-polymerase chain reaction. Open Access Maced J Med Sci, 2020; 8(A):146–52; doi:10.3889/oamjms.2020.3328

Sandfort F, Strieth-Kalthoff F, Kühnemund M, Beecks C, Glorius F. A structure-based platform for predicting chemical reactivity. Chem, 2020; 6:1379–90; doi:10.1016/j.chempr.2020.02.017

Shoombuatong W, Prathipati P, Prachayasittikul V, Schaduangrat N, Malik AA, Pratiwi R, Wanwimolruk S, Wikberg JES, Gleeson MP, Spjuth O, Nantasenamat C. Towards predicting the cytochrome P450 Modulation: from QSAR to proteochemometric modeling. Curr Drug Metab, 2017; 18; doi:10.2174/1389200218666170320121932

Song CM, Lim SJ, Tong JC. Recent advances in computer-aided drug design. Briefings Bioinform, 2009; 10:579–91.

Sumardi, Basyuni M, Wati R. Antimicrobial activity of polyisoprenoids of sixteen Mangrove species from North Sumatra, Indonesia. Biodiversitas, 2018; 19:1243–8; doi:10.13057/biodiv/d190409

Sychev DA, Ashraf GM, Svistunov AA, Maksimov ML, Tarasov VV, Chubarev VN, Otdelenov VA, Denisenko NP, Barreto GE, Aliev G. The cytochrome P450 isoenzyme and some new opportunities for the prediction of negative drug interaction in vivo. Drug Design Dev Ther, 2018; 12:1147–56.

Trehan I, Morandi F, Blaszczak LC, Shoichet BK. Using steric hindrance to design new inhibitors of class C β-lactamases. Chem Biol, 2002; 9(9):971–80.

Walum E. Acute oral toxicity. Environ Health Perspect, 1998; 106:497–503; doi:10.1289/ehp.98106497

Wang JL, Limburg D,Graneto MJ, Springer J, Hamper JRB, Liao S, Pawlitz JL, Kurumbail RG, Maziasz T, Talley JJ, et al. The novel benzopyran class of selective cyclooxygenase-2 inhibitors. Part 2: the second clinical candidate having a shorter and favorable human half-life. Bioorgan Med Chem Lett, 2010; 20:7159–63; doi:10.1016/j.bmcl.2010.07.054

Widiyana AP. Computation design of quinazoline-4(3H)-on derivatives as cyclooxygenase-2 (COX-2) inhibitor. Jurnal Farmasi Sains Dan Praktis, 2021; 7.

Widiyana AP, Putra GS, Muchlashi LA, Sulistyowaty MI, Budiati T. Design and molecular docking studies of quinazoline derivatives as antiproliferation. Jurnal Farmasi Dan Ilmu Kefarmasian Indonesia, 2016; 3(2):44–8.

Wu J, Xiao Q, Xu J, Li MY, Pan JY, Yang MH. Natural products from True Mangrove Flora: source, chemistry and bioactivities. Nat Prod Rep, 2008; 25:955–81.

Zhang R, Dong K, Wang Z, Miao R, Lu W, Wu X. Nanoparticulate drug delivery strategies to address intestinal cytochrome P450 Cyp3a4 metabolism towards personalized medicine. Pharmaceutics, 2021; 13.

How to cite this article:
Illian DN, Widiyana AP, Hasana AR, Maysarah H, Al Mustaniroh SS, Basyuni M. *In silico* approach: Prediction of ADMET, molecular docking, and QSPR of secondary metabolites in Mangroves. J Appl Pharm Sci, 2022; 12(11):021–029.